Journal of Surface Analysis Vol.15 No.3 (2009) pp. 216-219

Ion Beam Sputtering for High Resolution Depth Profiling

Hee Jae Kang,[1*] Dae Won Moon[2] and Hyung-Ik Lee[3]
[1]Department of Physics, Chungbuk National University, Cheongju, 361-763, Korea
[2]Korea Research Institute of Standards and Science, P.O.Box 102, Daejeon 305-600, Korea
[3]AE Center, Samsung Advanced Institute of Technology, POB 111, Suwon 440-600, Korea
[*]hjkang@cbu.ac.kr

(Received: January 19, 2009; Accepted: February 19, 2009)

The damage and the in-depth distributions of Argon atoms or Oxygen atoms in Si(100) surface after Ar^+ or O_2^+ ion beam sputtering were investigated by using Medium Energy Ion Scattering Spectroscopy and Dynamic Monte Carlo simulation. The primary ion energy was 0.5 keV and the primary ion beam direction was varied from surface normal to glancing angle. It was observed that the damage layer can be minimized with 0.5 keV O_2^+ and Ar^+ ion bombardments at the incident angle of 80^o from surface normal. In the case of 0.5 keV Ar^+ ion beam sputtering at the surface normal incidence, the maximum atomic concentration of Ar atoms was 6 at% at the depth of 2 nm, while at the incident angle of 80^o, the in-depth Ar distribution cannot be observed. In the case of 0.5 keV O_2^+ ion beam sputtering at surface normal incidence, the surface is continuously swelled to $\sim1.5\times10^{16}$ O_2^+ ions cm^{-2} ion dose owing to an incorporation rate of oxygen higher than the sputtering rate of Si. Dynamic Monte Carlo simulation reproduced the in-depth concentration distribution of Ar atoms and Oxygen atoms, quantitatively.

1. Introduction

Recently a low energy primary ion beam has been used to improve the depth resolution and to reduce the surface transient effect [1]. The ultimate limit for the depth resolution depends on how surface damage and transient width can be minimized during ion beam sputtering.

To minimize the surface damage effects caused by the ion beam sputtering is one of the key factors to obtain high resolution in sputter depth profiling. The surface transient effects caused by the implanted atoms during the ion beam sputtering at the initial stage of sputtering should be understood in order to analyze the depth profile of ultra thin films and the dopant profile of ultra shallow junctions. In this work, the damage and the in-depth distributions of the implanted atoms in Si(100) after 0.5 keV O_2^+ and Ar^+ ion bombardments have been studied by Medium Energy Ion Scattering Spectroscopy(MEIS)[2.3] and Dynamic Monte Carlo simulation[4].

2. Experiment

For the measurements of the damage profile, a MEIS analysis system connected with a ultrahigh vacuum chamber for ion beam sputter deposition and etching was used. A clean Si(100) surface was obtained by flashing up to 1150°C after etching with dilute HF. For the ion beam sputtering, 0.5 keV O_2^+ and Ar^+ ions were used. The current density of the ion beam was around 0.5 μAcm^{-2}, measured by Faraday cup moved to the sample position. During the ion beam sputtering, the pressure of the etching chamber is around 3.0×10^{-3} Pa. The MEIS analysis was done with 100 keV H^+ incident along the [111] direction and exiting along the [00-1] direction with the scattering angle of 125^0. Details of the MEIS techniques and the system used in this experiment were given elsewhere [2,3].

3. Results and discussion

The MEIS spectra taken from a clean Si (100) surface after saturation bombardment with 0.5 keV Ar^+ ion beam on Si surfaces are shown in Fig. 1. For comparison, the MEIS energy spectrum of an Si(100) surface is also shown. Because of the double alignment measurement condition, only Si atoms in the topmost atomic layer were measured, which yielded the surface peak before ion beam sputtering. As the incidence angle was changed from the surface normal to the grazing angle of 80^o, the height of the MEIS spectrum of damage peak increases, and the peak width showing the damage depth becomes wider as shown in Fig.1 (from 90.5 keV to 87 keV). It shows that the surface layer becomes amorphous, and the amorphous surface layer gets thicker as the incidence angle varied from glancing angle to surface normal. Details about the damage distribution can be seen elsewhere [5]. In this work, we focused on the quantitative analysis of the in-depth distribution of Ar from MEIS spectra as shown in Fig. 1 (right hand side peak).

The electronic energy loss factor estimated from the experimental condition is about 3.1nm/1000eV. Therefore the in-depth profile of the implanted Ar atoms can be estimated directly using the electronic energy loss.

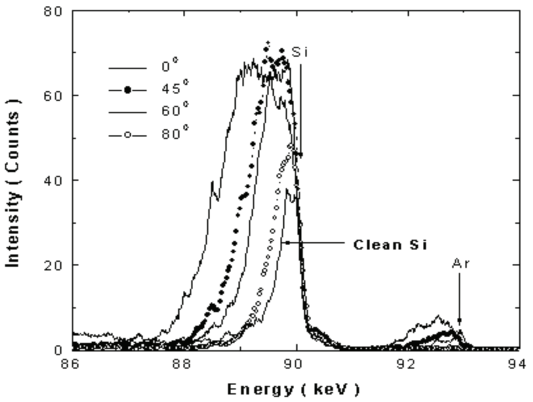

Fig. 1 MEIS spectra measured for the scattering angle of 125.3° after 0.5 keV Ar^+ ion beam sputtering on Si(100).

On the other hand, the atomic concentration can also be directly obtained from the peak heights of MEIS spectra with scattering cross section of Si and Ar. Figure 2 shows the concentration distribution of implanted Ar atoms after 0.5keV Ar ion sputtering obtained from the analysis of MEIS spectra and Monte Carlo simulation. The experimental result shows that the maximum concentration of implanted Ar atoms for the normal irradiation is 8 at% at about 2.0 nm from the surface, but at the incidence angle of 80°, there is no implanted Ar atom peak in the MEIS spectrum. It showed that the primary ion effects for sputter depth profiles can be minimized by using low energy at the incidence angle of 80°. Details about the in-depth distribution of the implanted Ar atoms can be seen elsewhere [5,6]. As can be seen in the figure, the damage thickness is closely related to the in-depth distribution of primary ion beam for sputtering.

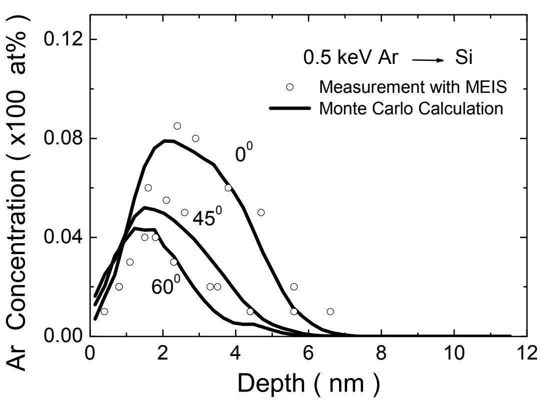

Fig. 2 In-depth distribution of Ar atoms in Si(100) after 0.5 keV Ar^+ ion beam sputtering on Si(100).

The MEIS energy spectra of Si(100) at the steady state after 500 eV O_2^+ ion beam sputtering at various incident angle are shown in Fig. 3. All the MEIS spectra were obtained after saturation ion dose. As the incident angle varies from surface normal to grazing incidence, the damaged layers become thinner and the total number of implanted oxygen decreases gradually. For 45°, the outermost atomic layer is fully oxidized but is partially oxidized for 60° as indicated in Fig. 4. The damaged layer thickness, measured from the Si peak, is reduced from 7.9 nm at the surface normal to 0.6 nm at the grazing incident angle of 80°. This shows that the sputter damage thickness is significantly reduced by low-energy and grazing incidence. But incident angle of 80° is not commonly used in AES, XPS and SIMS depth profiling because it is too difficult to focus the ion beam on the sample surface. The in-depth concentration profiles of oxygen at the steady stage for various incident angles are shown in Fig. 4. The MEIS experimental results, which were obtained from the MEIS damage profiles of Fig. 3, were compared with the simulation profiles. The simulation results for the incident angles of 0° and 45° show very good agreement with the MEIS experiments. For 60°, however, they show some discrepancy at the outermost layer because of oxygen flooding experimental condition. At the angle where the outermost layer is fully oxidized, oxygen flooding has no effect on the in-depth composition profile at the steady stages. At the angle where the outermost layer is partially oxidized, the in-depth composition profile under oxygen flooding is significantly varied because the outermost layer is fully oxidized due to oxygen flooding.

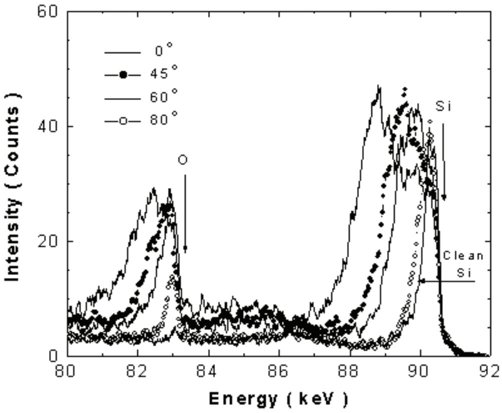

Fig. 3 MEIS spectra measured for the scattering angle of 125.3° after 0.5 keV O_2^+ ion beam sputtering on Si(100).

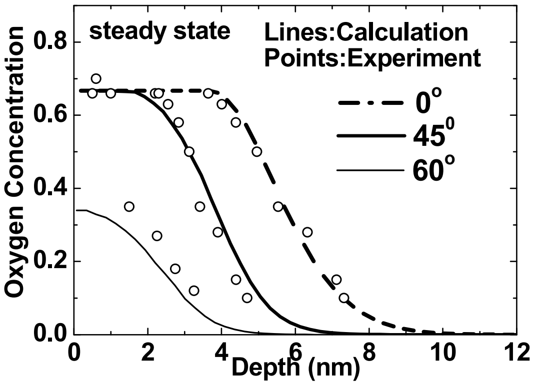

Fig. 4 The oxygen in-depth concentration profiles at the steady state for various incident angles. The MEIS experimental results (symbols) obtained from MEIS damage profiles of Fig. 3 were compared with simulation profiles (lines).

Figure 5 shows the MEIS damage profiles at various incident energies, which were obtained after the saturation ion dose. As the incidence energy decreases, the damaged layer becomes thinner and the total number of implanted oxygen atoms decreases gradually. The damaged layer thickness reduces from 7.9 nm at 500 eV to 4.9 nm at 100 eV. For the damage thickness, the MEIS results show clearly that the incidence angle effect is much larger than the energy effect for the low energy range of several hundred electron-volts. Therefore, to achieve high depth resolution, we should be considered to use low energy ion beam with the grazing incidence angle.

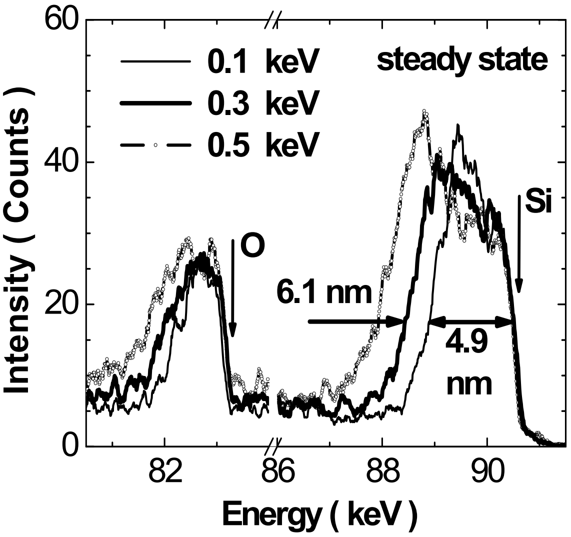

Fig. 5 MEIS spectra measured for the scattering angle of 125.3° after 0.1keV, 0.3keV and 0.5keV O_2^+ ion beam sputtering on Si(100) at surface normal incidence.

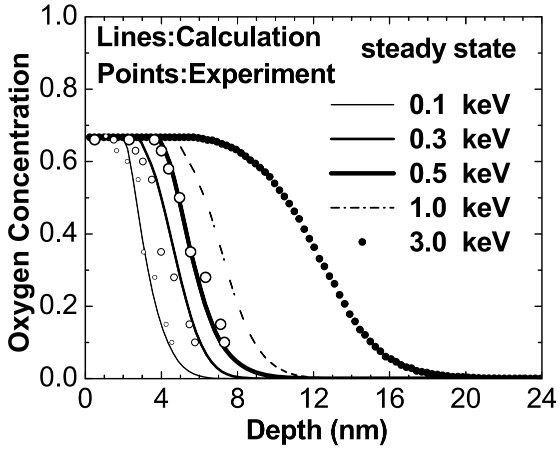

Fig. 6 The oxygen in-depth concentration profiles at the steady state for various incident energies. The MEIS experimental results (symbols) obtained from MEIS damage profiles of Fig. 5 were compared with simulation profiles (lines).

4. Conclusion

The damage and the in-depth distributions of implanted atoms in Si(100) and the change in sputtering yield on amorphous Si layers after 0.5 keV O_2^+ and Ar^+ ion beam sputtering have been studied by MEIS and dynamic Monte Carlo simulation. For 0.5 keV O_2^+ ion bombardment, the damage depth, measured from surface peak, was reduced from 7.9nm at surface normal incidence to 0.6nm at the glancing angle of 80° from surface normal. The surface composition at the damaged layer changed from Si at initial stage of sputtering to SiO_2 at the steady state. For 0.5 keV Ar^+ ion beam sputtering, the damage depth, measured from the surface peak, was reduced from 5.1nm at surface normal incidence to 0.5nm at the glancing angle of 80^o from surface normal. The maximum atomic concentration of implanted Ar atoms after 0.5 keV ion bombardments is about 8.0 at% at the depth of 2.0 nm for surface normal incidence, and the in-depth Ar distribution cannot be observed at the incident angle of 80^o from surface normal. The primary ion beam effect can be negligible when 0.5 keV Ar^+ ion bombardment with glancing angle of 80^o from surface normal incidence was used because the ion beam mixing effect caused by implanted Ar atoms can be neglected.

5. References

[1] Z.X. Jiang and P.F.A. Alkemade, Surf. Interface Anal. **27**, 125 (1999).
[2] J.C. Lee, C.S. Chung, H.J. Kang, Y.P. Kim, H.K. Kim, D.W. Moon, J. Vac. Sci. Technol. A**13,** 1325 (1995).
[3] D.H. Oh, H.J. Kang, K.H. Chae, C.N. Whang, B.V. King, D.J. O'Conor, D.W. Moon, Surf. Sci. **477**, L289 (2001).
[4] H.I. Lee, D.W. Moon, H.J. Kang, J. Appl. Phys. **99**, 123507 (2006).
[5] D.W. Oh, S.K. Oh, H.J. Kang, H.I. Lee, D.W. Moon, Nucl. Instr. and Meth. **B 190**, 598 (2002).
[6] H.I. Lee, H.K. Kim, K.J. Kim, D.W. Moon, H.K. Shon, H.C. Shin, H.J. Kang, Surf. Interface Anal. **36**, 295 (2004).